Modelling Deformation-induced Precipitation Kinetics in Microalloyed Steels during Hot Rolling

Zhanli Guo[1,a] and A.P. Miodownik[1]

[1]Sente Software Ltd., Surrey Technology Centre, Guildford GU2 7YG, U.K.

[a]z.guo@sentesoftware.co.uk

Keywords: Microalloyed steels, Precipitation kinetics, Hot rolling, Deformation.

Abstract. This paper reports the framework of a computer model that calculates the precipitation kinetics of MX type carbides or carbonitrides from austenite matrix in microalloyed steels during hot rolling. The kinetic model is based on the classical Johnson-Mehl-Avrami theory adapted to include the saturation of nucleation sites. The effect of deformation on precipitation kinetics is quantitatively described through its effect on flow stress, from which the number of potential nucleation sites can be estimated. The time-temperature precipitation diagram can then be calculated for a given alloy chemistry and deformation conditions. A preliminary study has been carried out to test its performance in both undeformed and deformed conditions.

Introduction

Deformation-induced precipitation (DIP) takes place in microalloyed steels during hot rolling. DIP holding is placed between the initial rough rolling phase and further rolling passes to allow MX type carbides, nitrides and/or carbonitrides (referred to generally as carbonitrides in what follows) to form in the austenite matrix, which in turn retard or suppress recrystallisation during further rolling. The accumulated strain and deformed structures of austenite grains can therefore be retained, leading to a high nucleation rate for ferrite or other transformation products during subsequent transformation. Thus the precipitation of MX particles plays an important role in controlling the final microstructure and hence the properties of the products, and it is essential to understand the mechanisms of precipitation during the hot rolling of microalloyed steels.

Extensive experimental studies of the precipitation kinetics of MX carbonitrides conclusively show that prior deformation enhances the precipitation kinetics significantly.[1,2,3,4,5,6,7] However, these studies involve a large number of variables such as steel composition, initial grain size, and deformation condition (temperature, amount of strain, strain rate and type of deformation). As a result, it is difficult to make a meaningful comparison of all the experimental results and shed light on the directions for improvement. Modelling approaches that investigate specific variables offer a possible solution. An early attempt was made by Dutta and Sellars,[8] who proposed a model to predict the precipitation start (corresponding to 5% precipitation) time for Nb steels. Although this model is simple and shows reasonably good agreement with many of the experimental data, it does not consider the complete precipitation kinetics, i.e. the evolution of precipitate volume fraction and size with time. A similar model was proposed by Liu and Jonas for microalloyed steels containing Ti or Nb.[9,10] Although this model considers the heterogeneous nucleation of precipitates on dislocations, it does not consider the precipitate coarsening, which was observed by Dutta et al.[11]

The most comprehensive model up to date was developed by Dutta et al.,[12] where the precipitation kinetics considers the nucleation, growth and coarsening of precipitates and the early occurrence of coarsening. A significant step forward made by this model is its estimation of nucleation number density from flow stress via the estimation of dislocation density. Although an excellent model, it suffers from two critical drawbacks that prevent it from being predictive. On the one hand, the thermodynamic description of MX carbonitride is based on the concept of solubility product, which is not readily applicable to complex M(C,N) precipitates, where M can be Nb, Ti and V or a mixture of the three elements. On the other hand, a fitting parameter defined as a "dislocation

density factor" has to be used to account for the effect of different deformation conditions on dislocation density and its value can only be obtained by fitting against experimental results.

This paper describes a technique using the materials modelling tool JMatPro,[13] which is capable of calculating flow stress as a function of strain, strain rate and temperature as well as alloy composition and grain size. The necessity of such a "dislocation density factor" is therefore removed. In addition, the thermodynamic solver built into JMatPro is based on the CALPHAD approach,[14] which can more accurately deal with the thermodynamics of complex MX carbonitrides. Hence it is now possible, for the first time, to calculate the deformation-induced precipitation kinetics of MX formation in an austenite matrix of selected composition combined with a selected hot rolling scheme. The first part of the paper describes the crucial steps of the model development. The second part features parameter assessment and the calculation of time-temperature precipitation (TTP) curves for four microalloyed steels, followed by discussions on further improvements.

Model Development

To be able to make prediction of the MX precipitation in a combination of alloy composotion, deformation and heat-treatment, the model should contain the following crucial elements:

1. A thermodynamics tool to calculate the thermodynamics of a complex MX phase.
2. A treatment of precipitation kinetics which includes nucleation, growth and coarsening.
3. Flow stress calculation as a function of alloy composition and deformation condition.
4. A link between flow stress and the number of potential nucleation sites.

Thermodynamic calculation via a CALPHAD approach has been a mature technique for decades and is particularly important when dealing with multi-component systems.[14] Such calculatiion can provide information such as phase fraction and constituents as well as the driving force for a transformation and are a standard feature of JMatPro. Assessment of such calculation has been carried out during the development of thermodynamic databases and is not discussed here.

Precipitation kinetics. The precipitation kinetics of MX is described using a modified Johnson-Mehl-Avrami (JMA) model, which has been previously presented.[15] So only the key features are presented here. For the case of steady state nucleation, the governing equation is written as:

$$X = \frac{V}{V_{eq}(T)} = 1 - \exp\left(- f \frac{l_c^{3-p}}{p+1} N_r G_r^p t^{p+1} \right) \quad (1)$$

where X is the volume percentage of the product phase; V is the volume fraction transformed; $V_{eq}(T)$ is the equilibrium fraction at temperature T; f is a shape factor; l_c is a 'critical dimension'; p is a value related to the dimension of growth; N_r is the nucleation rate; G_r is the growth rate and t is time. For the case where site saturation occurs, one has:

$$X = 1 - \exp\left(- f l_c^{3-p} N_0 G_r^p t^p \right) \quad (2)$$

where N_0 is the total number of active nucleant sites per unit volume, i.e. the saturation number density. Eqs. 1 and 2 are isothermal in nature and can be used directly to calculate the evolution of phase fraction vs. time at a constant temperature or various temperatures, i.e. TTP diagrams.

The nucleation rate N_r in the present work was obtained by modifying the previous equations used by Saunders and Miodownik[16] for nucleation from the liquid by the inclusion of X_α:[17]

$$N_r = \frac{N_0 D X_\alpha}{a_0^2} \exp\left(- \frac{16\pi\alpha^3}{3NkT_P} f(\theta) \frac{\Delta H_m^3}{\Delta G_m^2} \right) \quad (3)$$

where D is the diffusion coefficient; X_α is the relevant solute concentration in matrix [e.g. X_{Nb} for Nb in austenite]; a_0 is atomic spacing; k is Boltzman's constant; T_P is the precipitation temperature; N is Avagadro's number; α is a constant relating ΔH_m to the matrix/nucleus interfacial energy; and θ is an effective wetting angle, and $f(\theta)=(2-3\cos\theta+\cos^3\theta)/4$. ΔH_m and ΔG_m are the enthalpy and molar Gibbs energy driving force of transformation, respectively. The growth rate can be calculated using the following equation:[15,18]

$$G_r = \kappa D\left[\frac{\Delta G_m}{RT}\right] \tag{4}$$

where κ is a constant, whose value is in the order of 10^7 to 10^8. Of all the parameters involved in the above equations, the number of potential sites for nucleation, N_0, is of particular importance in deformation induced precipitation, and its estimation is given below.

Calculation of N_0. Deformation affects precipitation kinetics via its effect on the number of potential nucleation sites. On the basis that all the dislocation nodes act as potential nucleation sites for MX precipitation, the number of potential sites per unit volume can be calculated as:[19,20]

$$N_0 = 0.5\rho^{1.5} \tag{5}$$

where ρ is the dislocation density, which can be estimated as:

$$\rho = \left(\frac{\sigma - \sigma_y}{\alpha M \mu b}\right)^2 \tag{6}$$

where σ and σ_y are the flow stress and yield stress at the deformation temperature T_{def}, respectively. M is Taylor factor (3.1 for F.C.C. crystals), α is a constant, μ is the shear modulus and b is the Burgers vector. The estimation of N_0 now becomes a problem of how to calculate flow stress as a function of temperature and deformation conditions, which is briefly explained below.

Calculation of flow stress. Depending on the temperature and strain rate regime, the flow stress curve may take on various shapes as a result of working hardening or flow softening.[21] When only work (strain) hardening is in operation, stress is related to strain and strain rate via work hardening coefficient n and strain rate sensitivity m, respectively:

$$\sigma = K\varepsilon^n \dot{\varepsilon}^m \tag{7}$$

where K is a constant. The value of n can be estimated from yield stress σ_y via:

$$n = a\exp(b\sigma_y) \tag{8}$$

where a and b are material constants dependent of alloy type. Their values have been fitted for a wide range of austenitic steels.[22] Details on the flow stress model are given in Ref. 21. When the room temperature yield stress of austenite is known, its temperature dependence is determined by following the procedures described in previous work.[23]

Model Assessment

To use Eqs. 1 to 4 to perform the calculation of precipitation kinetics, the values of $V_{eq}(T)$, X_α, ΔH_m and ΔG_m have first to be obtained via thermodynamic calculations.[15] The specific parameters for MX precipitation such as f, p, α, l_c, θ, and κ have to be evaluated mainly based on matching the experimental results, which can then be used for a whole range of compositions. There also exists a self-consistent diffusion database inside JMatPro for the calculation lattice diffusion coefficient.

Calculation of flow stress and estimation of nucleation density. Rainforth et al. studied the precipitation of NbC in an Fe-30Ni-0.1C-0.1Nb-1.61Mn (wt.%) steel of initial grain size 370 μm.[24] The nucleation number density is observed to be 3.8×10^{21} m^{-3} after deformation at 950°C to give a strain 0.5 at strain rate 10 s^{-1}. To calculate the flow stress curve, JMatPro first calculates the strength of austenite as a function of temperature at strain rate 10 s^{-1}, Fig. 1. The yield stress at 950°C at this rate is 101.5 MPa and shear modulus is 48.7 GPa. The calculated flow stress curve is compared with the experimental data, Fig. 2. The only unknown parameter in Eqs. 6 and 7 is α, which is estimated to be 0.22 to fit the observed nucleation number density, close to the value 0.15 quoted in Ref. 12. This value is used in the present study.

Calculation of TTP curves. Four steels were chosen to test this treatment, with experimental work drawn from various sources.[1,2,5] Their compositions are given in Table 1, together with deformation conditions and the calculated yield stress, flow stress, dislocation density and number of nucleation density.

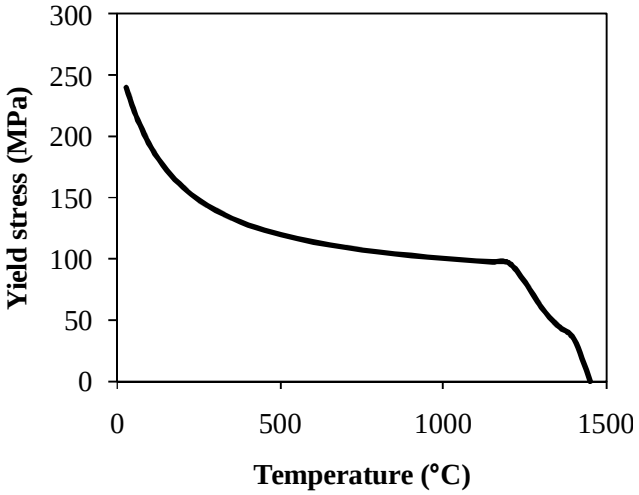

Fig. 1. Yield stress of austenite as a function of temperature calculated at strain rate 10 s^{-1}.

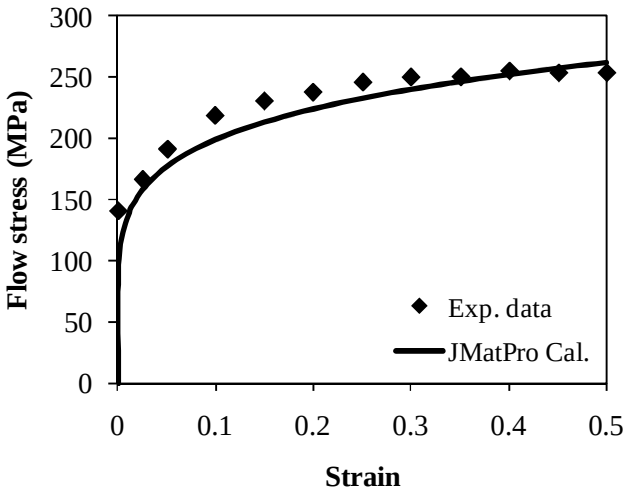

Fig. 2. Flow stress curve at 950°C at strain rate 10 s^{-1}, experimental data from Ref. 24.

Table 1. Alloy information, deformation conditions and some estimated parameters.

Alloy composition	Deformation conditions	σ_y [MPa]	σ [MPa]	ρ [m^{-2}]	N_0 [m^{-3}]	Ref.
Fe-0.17C-0.011N-0.04Nb-1.35Mn-0.31Si	Annealed at 1260°C, undeformed*	56.5	71.0	6.3×10^{12}	7.8×10^{18}	Le Bon[1]
Fe-0.063C-0.0058N-0.084Nb	Annealed at 1300°C, undeformed*	29.7	64.3	3.1×10^{13}	8.5×10^{19}	Watanabe[2]
Fe-0.11C-1.35Mn-0.26Si-0.031Nb-0.01N	Annealed at 1100°C, deformed at 950°C, 50% reduction at 2.60 s^{-1}**	43.3	270.0	1.3×10^{15}	2.3×10^{22}	Steel2[5]
Fe-0.10C-1.24Mn-0.23Si-0.095Nb-0.01N	Annealed at 1250°C, deformed at 950°C, 50% reduction at 2.60 s^{-1}**	40.7	260.0	1.2×10^{15}	2.1×10^{22}	Steel3[5]

* 950°C was used for flow stress calculation and nucleation density estimation.

** The strain rate was not given in the original paper, so here used the value quoted in Ref. 8.

Figs. 3 and 4 are the calculated MX molar fraction and the amount of Nb in austenite as a function of temperature in the four steels. As can been see that the MX solvus temperatures differ significantly. It should be noted that the annealing temperatures for Steel 2 and Steel 3 seem not to be high enough to completely dissolve MX into the austenite matrix.

The calculated TTP curves of the four steels are shown in Fig. 5. When temperature decreases to around 850°C, ferrite will become a stable phase and the matrix will be no longer 100% austenite. MX may still form from austenite but the calculation is not carried out in this study. A maximum

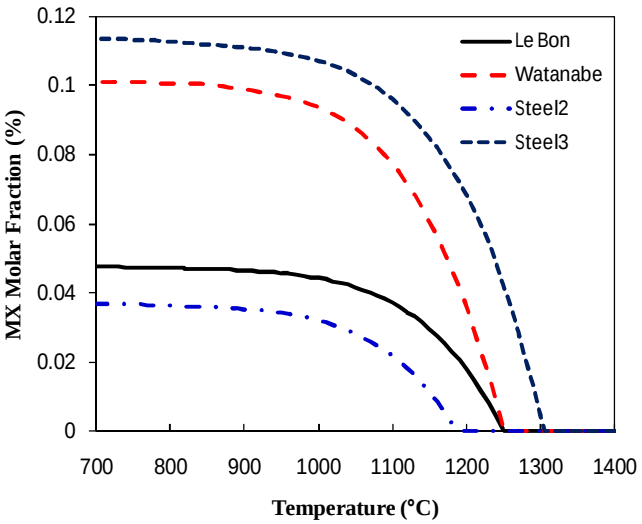

Fig. 3. Molar fraction of MX in the fours steels calculated using JMatPro.

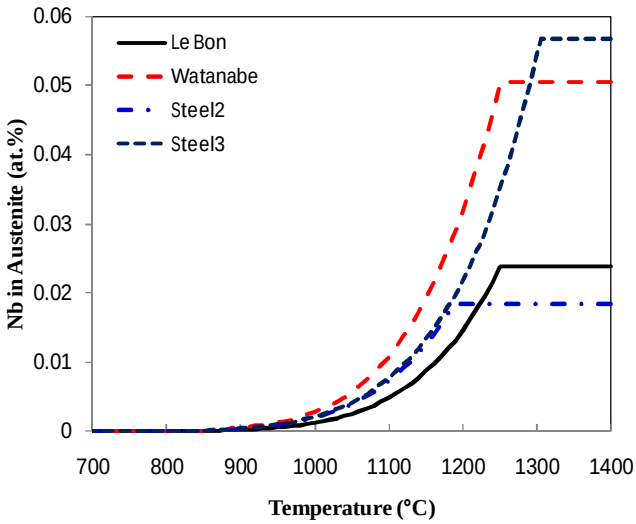

Fig. 4. Nb in austenite in the fours steels calculated using JMatPro.

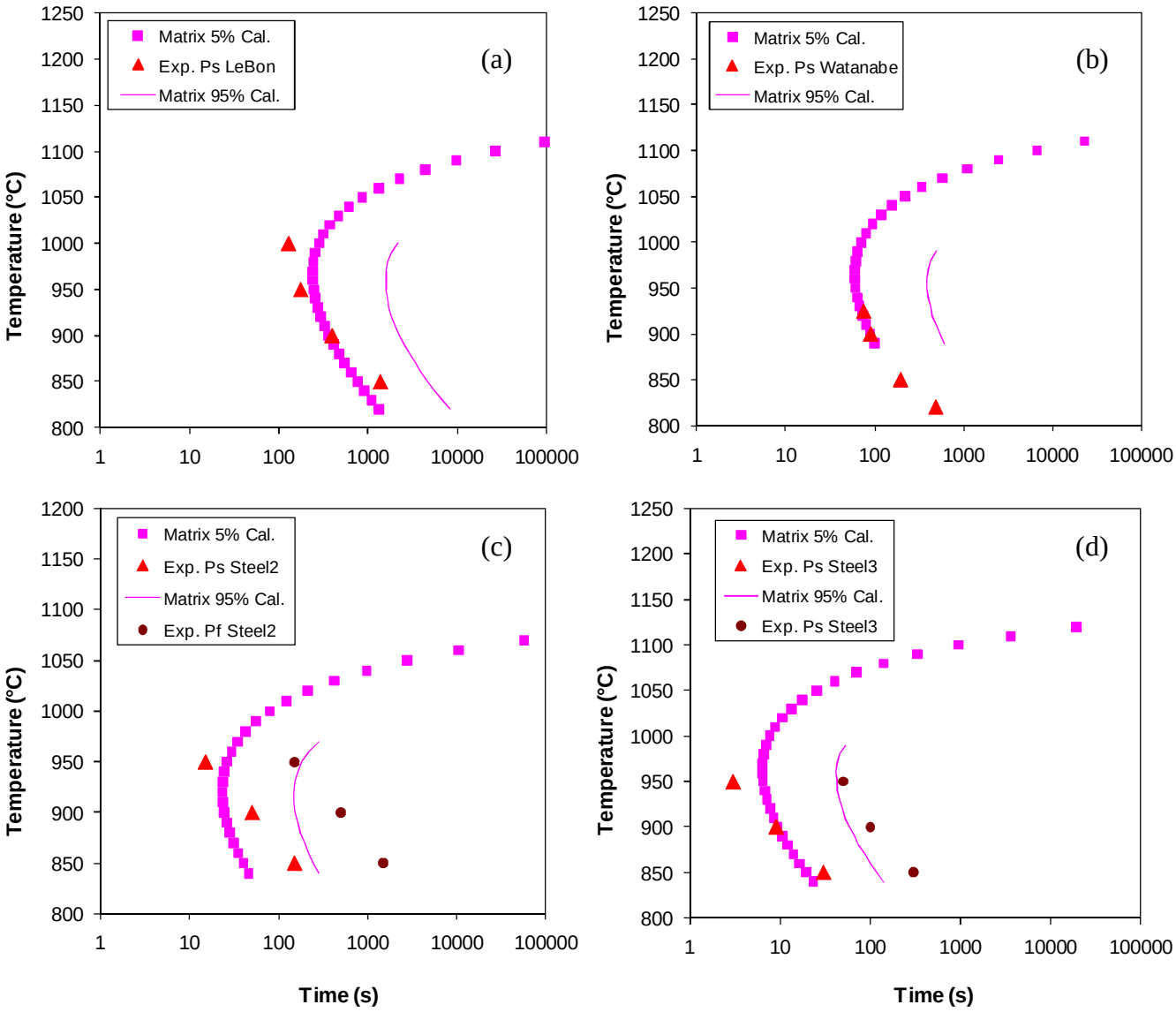

Fig. 5. Calculated TTP curves for four microalloyed steels in comparison with the experimental data from: (a) Le Bon,[1] (b) Watanabe,[2] (c), Steel2 of Hansen et al,[5] and (d) Steel3 of Hansen et al.[5]

equilibrium fraction, V_{eq_max}, is shown in Fig. 3 for each alloy. The 5% start curve (Ps) or 95% completion curve (Pf) correspond to that of V_{eq_max}. So each point on the Ps or Pf curves corresponds to the same absolute fraction. No completion curve is given for temperatures at which V_{eq} is lower than 95% of V_{eq_max}.

The overall agreement for the four alloys are acceptable, which demonstrates the potential of this approach. However there are many factors not yet considered which would improve matters further:

- Particle coarsening needs to be included as the reduction in the number of precipitates would lead to a slowing-down in the precipitation kinetics, especially the completion time. Particle coarsening has already been considered in the context of other heat-treatment procedures.[25]
- Dislocation pipe diffusion has not been included but, depending on temperature, could contribute to the precipitation growth and coarsening via accelerated diffusion process.
- Reduction of driving force during transformation, which may slow down the precipitation kinetics. This has been considered previously in the context of other heat-treatments.

It is intended to extend the treatment to include isothermal precipitation kinetics, where information on particle size will be calculated along with its volume fraction.

Summary

A model that can predict the precipitation kinetics of MX formation from the austenite matrix in

microalloyed steels during hot rolling has been developed in the present study. The core of the present approach is the estimation of the dislocation density and the number density of potential nucleants using JMatPro to extract the relevant information from calculated flow stress curves in addition to calculating the basic phase equilibria. The significant advantage of this model over previous ones is that it can be applied to alloys of any desired chemistry under a wide range of "virtual" deformation conditions.

Acknowledgements

The authors gratefully acknowledge Dr. Nigel Saunders and Dr. Jean-Philippe Schillé for useful discussions in preparation of this paper.

References

[1] A. le. Bon, J. Rofes-Vernis and C. Rossard: Metal Science Vol. 9 (1975), p.36
[2] A. Watanabe, Y.E. Smith and R.D. Pehlka, in: Hot Deformation of Austenite, J.B. Balance ed., The Metallurgical Society of AIME, New York, 140-168 (1977).
[3] R. Simoneau, G. Begin and A.H. Marquis: Metal Science Vol. 12 (1978), p. 381
[4] I. Weiss and J.J. Jonas: Metall. Trans. A Vol. 10A (1979), p. 831
[5] S.S. Hansen, J. B. Vander Sande and M. Cohen: Metall. Trans. A Vol. 11A (1980), p. 387
[6] C.S. Janampa: Ph.D. thesis, The University of Sheffield, 1982.
[7] C. Iparraguirre, A.I. Fernández, B. López, C. Scott, A. Rose, W. Kranendonk, B. Soenen and G. Paul: Materials Science Forum Vols. 500-501 (2005), p. 677
[8] B. Dutta and C.M. Sellars: Mat. Sci. Technol. Vol. 3 (1987), p. 197
[9] W.J. Liu and J.J. Jonas: Metall. Trans. A Vol. 20A (1989), p. 689
[10] W.J. Liu: Metall. Mater. Trans. A, Vol. 26A (1995) p. 1641
[11] B. Dutta, E. Valdes and C.M. Sellars: Acta Metall. Mater. Vol. 40 (1992), p. 653
[12] B. Dutta, E.J. Palmiere and C.M. Sellars: Acta Mater. Vol. 49 (2001), p. 785
[13] Z. Guo, N. Saunders, A.P. Miodownik and J-Ph. Schillé: Mater. Sci. Eng. A Vol. 499A (2009), p. 7
[14] N. Saunders and A.P. Miodownik: *CALPHAD – Calculation of Phase Diagrams*, Pergamon Materials Series Vol.1, ed. R.W. Cahn, (Oxford, Elsevier Science, 1998).
[15] X. Li, A.P. Miodownik and N. Saunders: Mater. Sci. Technol. Vol. 18 (2002), p. 861
[16] N. Saunders and A.P. Miodownik: Mater. Sci. Technol. Vol. 4 (1988), p. 768
[17] N. Saunders and P. Tsakiropoulos: Mater. Sci. Technol. Vol. 4 (1988), p. 157
[18] J.W. Martin, R.D. Doherty and B. Cantor: *Stability of Microstructure in Metallic Systems* (Cambridge University Press, Cambridge, 1997).
[19] B. Dutta, E. Valdes and C.M. Sellars: Acta Metall. Mater. Vol. 40 (1992), p. 653
[20] B. Dutta, E.J. Palmiere and C.M. Sellars: Acta Mater. Vol. 49 (2001), p.785
[21] Z. Guo, N. Saunders, J.P. Schillé and A.P. Miodownik, in: MRS International Materials Research Conference, 9-12 June 2008, Chongqing, China
[22] Unpublished research, Sente Software Ltd., 2003.
[23] Z. Guo, N. Saunders, A.P. Miodownik and J.P. Schillé: Materials Science Forum Vols.546-549 (2007), p. 1319
[24] W.M. Rainforth, M.P. Black, R.L. Higginson, E.J. Palmiere, C.M. Sellars, I. Prabst, P. Warbichler and F. Hofer: Acta Materialia Vol. 50 (2002), p. 735
[25] N. Saunders, Z. Guo, A. P. Miodownik and J-Ph. Schillé: Modelling High Temperature Mechanical Properties and Microstructure Evolution in Ni-based Superalloys, Internal report, Sente Software Ltd. (2008)